Direction of amygdala–neocortex interaction during dynamic facial expression processing

Running head: Amygdala–neocortex interaction for dynamic faces

Wataru Sato[1,†], Takanori Kochiyama[2,†], Shota Uono[1], Sakiko Yoshikawa[3], and Motomi Toichi[4]

[1] Department of Neurodevelopmental Psychiatry, Habilitation and Rehabilitation, Graduate School of Medicine, Kyoto University. [2] Brain Activity Imaging Center, Advanced Telecommunications Research Institute International. [3] Kokoro Research Center, Kyoto University. [4] Faculty of Human Health Science, Graduate School of Medicine, Kyoto University. [†] Equal contributors.

Corresponding author

Wataru Sato. Department of Neurodevelopmental Psychiatry, Habilitation and Rehabilitation, Graduate School of Medicine, Kyoto University, 53 Shogoin-Kawaharacho, Sakyo, Kyoto 606-8507, Japan. E-mail: sato.wataru.4v@kyoto-u.ac.jp

Abstract

Dynamic facial expressions of emotion strongly elicit multifaceted emotional, perceptual, cognitive, and motor responses. Neuroimaging studies revealed that some subcortical (e.g., amygdala) and neocortical (e.g., superior temporal sulcus and inferior frontal gyrus) brain regions and their functional interaction were involved in processing dynamic facial expressions. However, the direction of the functional interaction between the amygdala and the neocortex remains unknown. To investigate this issue, we re-analyzed functional magnetic resonance imaging (fMRI) data from two studies and magnetoencephalography (MEG) data from one study. First, a psychophysiological interaction analysis of the fMRI data confirmed the functional interaction between the amygdala and neocortical regions. Then, dynamic causal modeling analysis was used to compare models with forward, backward, or bi-directional effective connectivity between the amygdala and neocortical networks in the fMRI and MEG data. The results consistently supported the model of effective connectivity from the amygdala to the neocortex. Further increasing time-window analysis of the MEG demonstrated that this model was valid after 200 ms from the stimulus onset. These data suggest that emotional processing in the amygdala rapidly modulates some neocortical processing, such as perception, recognition, and motor mimicry, when observing dynamic facial expressions of emotion.

Keywords

Amygdala; Dynamic causal modeling; Dynamic facial expression; Inferior frontal gyrus; Psychophysiological interaction.

Introduction

Dynamic facial expressions of emotion are indispensable communicative media for human social interactions, because emotional facial expressions are the primary source of messages (Mehrabian, 1971) and normal facial expressions are dynamic (Darwin, 1872). Behavioral studies have revealed that dynamic facial expressions trigger multiple strong psychological responses. For example, previous studies showed that the observation of dynamic facial expressions elicited stronger subjective emotional experiences compared with static facial expressions or dynamic mosaics (Sato and Yoshikawa, 2007b). The emotional effects of dynamic facial expressions were processed rapidly, even before conscious awareness of the faces (Sato et al., 2014). Other studies revealed that dynamic, compared to static, facial expressions induced perceptual enhancement (Yoshikawa and Sato, 2008), more accurate recognition of emotion (Bould et al., 2008), and more evident facial mimicry (Sato and Yoshikawa, 2007a).

Neuroscience studies have uncovered the neural mechanism for such effective processing of dynamic facial expressions. Neuroimaging studies using functional magnetic resonance imaging (fMRI) and positron emission tomography compared brain activation as participants observed dynamic facial expressions and control stimuli, such as static facial expressions and dynamic mosaics (e.g., LaBar et al., 2003; Sato et al., 2004; for a review, see Arsalidou et al., 2011). The studies consistently found activity in some subcortical regions, such as the amygdala, and some cortical regions, including the V5/middle temporal area (MT), fusiform gyrus (FG), superior temporal sulcus region (STS) including the adjacent middle and superior temporal gyri (cf. Allison et al., 2000), and the inferior frontal gyrus (IFG). Substantial neuroimaging and neuropsychological evidence suggested that the activation of these brain regions was consistent with their information processing functions, such as emotional processing involving the amygdala (Calder et al., 2001), visual analysis of the dynamic aspects of faces (Allison et al., 2000), recognition of the inner states of others involving the STS (Frith, 2001), and motor mimicry involving the IFG (Iacoboni, 2005). Some electrophysiological studies employing electroencephalography (EEG), magnetoencephalography (MEG), or intracranial EEG further revealed the temporal profiles of activities in these brain regions during dynamic facial expression processing (e.g., Tsuchiya et al., 2008; Sato et al., 2015). For example, Sato et al. (2015) revealed that the visual areas (V5/MT, FG, and STS) and IFG were activated at 150–200 and 300–350 ms, respectively, in response to dynamic facial expressions versus dynamic mosaics.

Furthermore, a previous fMRI study increased the mechanistic understanding of dynamic facial expression processing by showing functional interactions among brain regions (Foley et al., 2012). In that study, psychophysiological interactions (PPIs) (Friston et al., 1997; Gitelman et al., 2003) were analyzed during the observation of dynamic and static facial expressions using fMRI data. PPI analysis reveals how activity in a particular brain region is differentially correlated (i.e., functionally interacts) with that in other brain regions depending on the experimental conditions (Friston et al., 1997; Gitelman et al., 2003). Compared with the observation of static facial expressions, that of dynamic facial expressions induced more functional interaction between the amygdala and some neocortical regions, including the FG, STS, and IFG. Such functional interaction is consistent with

the anatomical evidence indicating white matter connectivity between the amygdala and the visual/motor regions in non-human primates (Amaral and Price, 1984; Avendano et al., 1983; for a review, see Amaral et al., 1992) and humans (Catani et al., 2003; Grèzes et al., 2014). Taken together, these neuroimaging and electrophysiological findings indicate that processing observed during dynamic facial expressions induces rapid activity and functional interactions in the amygdala and neocortical regions.

However, the direction of the interaction by which the amygdala and neocortex could interact during dynamic facial expression processing in the neural network remains unclear, because PPI analysis does not provide causal information about the directional influences among regions. This question can be answered by investigating the effective connectivity among brain regions using a dynamic causal modeling (DCM) approach (Friston et al., 2003; Friston, 2011). This question is important because different direction interactions among brain regions could have different functional implications. Specifically, an influence of the amygdala on the neocortex would suggest that emotional processing modulates perceptual, cognitive, and/or motor processing of dynamic facial expressions (we call this the "directional connectivity from the amygdala" model). In contrast, an influence of the neocortex on the amygdala would imply that perceptual, cognitive, and motor responses influence emotional processing (we call this the "directional connectivity to the amygdala" model). The direction of this influence has implications for understanding the processing of emotional facial expressions, as well as the general relationship between emotion and cognition (cf. Zajonc, 1980; Lazarus, 1982). Several studies theoretically proposed that the amygdala may conduct rapid emotional processing for facial expressions and modulate activities in the neocortical regions (e.g., Adolphs, 2001; Vuilleumier and Pourtois, 2007; Sato et al., 2013), because anatomical studies in non-human primates showed that the amygdala receives visual input via subcortical pathways (involving the superior colliculus and pulvinar), bypassing the neocortical visual areas (Day-Brown et al., 2010), and sends projections to widespread neocortical regions, including the visual and motor areas (Amaral and Price, 1984; Avendano et al., 1983; for a review, see Amaral et al., 1992). Anatomical neuroimaging studies confirmed the white matter connections of the amygdala–pulvinar–superior colliculus (Rafal et al., 2015; Tamietto et al., 2012) and amygdala–visual/motor neocortices (Catani et al., 2003; Grèzes et al., 2014) in humans. A previous intracranial EEG study also reported that activation of the amygdala in response to static emotional facial expressions was rapid, which could occur prior to neocortical activities (Sato et al., 2011). A previous study that applied DCM to fMRI data also reported significant modulatory effects from the amygdala on neocortical regions, including the STS and IFG, but not in the reverse direction (Grèzes et al., 2009), although their stimuli were dynamic body gestures without facial information. Based on these data, we hypothesized that the direction of the amygdala–neocortex interaction during the processing of dynamic facial expressions could be from the amygdala to the neocortex.

Furthermore, it remains unknown specifically when the amygdala–neocortex interaction could occur. This question is important because neural events at different time stages reflect different psychological functions. Even if we assumed that the causal direction was from the amygdala to the neocortex, the amygdala might modulate the neocortex slowly via some indirect efferent routes that take ≥1 s longer, such as projections from the nucleus reticularis pontis caudalis of the brainstem (cf.

Steriade et al., 1993). However, several previous scalp EEG studies reported that the effects of emotional facial expressions on neocortical activities, which were likely derived from amygdala modulation, occurred at 200–400 ms (e.g., Balconi and Pozzoli, 2003; Sato et al., 2001; Sawada et al., 2014). Based on these data, we hypothesized that modulation from the amygdala to the neocortex would be implemented during the first few hundred milliseconds, specifically at 200–400 ms.

To investigate these hypotheses, we re-analyzed the fMRI data obtained from two studies (study 1: Sato et al., 2004; study 2: Sato et al., 2012) and MEG data from one study (Sato et al., 2015). In all three studies, brain activity was measured during the observation of dynamic facial expressions without explicit emotion-recognition tasks. We first analyzed the fMRI data and confirmed regional brain activity by identifying activation foci. Then, we performed PPI and confirmed the functional interaction between the amygdala and the neocortical regions. We then conducted DCM analyses (Friston et al., 2003). We compared models of intrinsic and modulatory effective connections from the amygdala to the neocortex, from the neocortex to the amygdala, or both. We also conducted DCM using similar model comparisons for the MEG data. Finally, we conducted an increasing time-window analysis of the DCM for the MEG data (Garrido et al., 2007; Garrido et al., 2012) to identify the time stage that the model fitted.

Materials and Methods

Participants

Data were collected from 22 participants in fMRI study 1 (12 females; mean age, 26.5 years), 13 participants (1 female; mean age, 24.3 years) in fMRI study 2, and 15 participants (6 females; mean age, 26.9 years) in the MEG study. All participants were Japanese, right-handed, and had normal or corrected-to-normal visual acuity. Written informed consent was obtained from all participants after the experimental procedures had been fully explained. The studies were conducted in accordance with the institutional ethical provisions.

Stimuli

The dynamic facial expression stimuli in all studies consisted of morphing animations. The raw materials were grayscale photographs of the faces of eight individuals (4 females) depicting fearful, happy, and neutral expressions selected from a standard set of images (Ekman and Friesen, 1976). Neutral expressions were adopted as the starting point of the emotional expressions. Between the neutral (0%) and emotional (100%) expressions, 24 intermediate images (increments of 4%) were created using morphing software (FUTON System, ATR). The images were presented in succession as a moving clip. Each clip was presented for 1,500 ms (40 ms for 0–100%, and an additional 230 ms for 0 and 100%) in fMRI studies 1 and 2, and for 500 ms (20 ms for 4–100%) in the MEG study. A previous behavioral study confirmed that these speeds sufficiently reflected the natural changes that occur in dynamic facial expressions of fear and happiness (Sato and Yoshikawa, 2004).

As control stimuli, static expressions (the final expressions under the dynamic expression condition) were used in fMRI studies 1 and 2. Dynamic mosaics in which the frames of the dynamic facial expressions were divided into 18 vertical × 12 horizontal squares, reordered randomly using a constant algorithm, and presented as moving clips were used in the MEG study. Although the dynamic mosaic images were also presented in fMRI study 1, we analyzed only the data from the static facial expressions to allow us to combine the data from both fMRI studies.

The stimuli subtended visual angles of 15.0° vertical and 10.0° horizontal in all studies. Previous behavioral studies confirmed that these dynamic facial expressions and control stimuli elicited different patterns of subjective emotional responses (Sato and Yoshikawa, 2007b) and facial mimicry (Sato and Yoshikawa, 2007a).

Procedure

In all studies, the participants observed the dynamic facial expressions and control stimuli without explicit emotion-recognition tasks. In fMRI study 1, participants were instructed to observe the images carefully while fixating on the center of the screen. In fMRI study 2, participants were asked to specify the stimulus gender by pressing one of two buttons using the left or right forefingers. In the MEG study, participants were instructed to detect dummy targets (red cross) by pressing a button with their right forefinger.

In each trial of all the studies, each stimulus was presented after a fixation point shown for 1,500, 1,000, and 500 ms for fMRI study 1, fMRI study 2, and the MEG study, respectively. Participants observed a total of 40, 96, and 112 dynamic facial expressions and the same number of control stimuli in fMRI study 1, fMRI study 2, and the MEG study, respectively. In fMRI studies 1 and 2, a block design was adopted using 30-s and 20-s epochs, respectively. For the MEG study, an event-related design was adopted. The order of stimuli was pseudorandomized in all studies.

MRI acquisition

In fMRI study 1, image scanning was performed using a 1.5-T scanning system (Magnex Eclipse 1.5T Power Drive 250, Shimadzu Marconi, Kyoto, Japan) at the ATR Brain Activity Imaging Center using a standard radio frequency head coil for signal transmission and reception. The functional images consisted of 52 consecutive slices parallel to the anterior–posterior commissure plane covering the whole brain. A T2*-weighted gradient-echo echo planar imaging sequence was used with the following parameters: repetition time (TR)/echo time (TE) = 6,000/60 ms; flip angle (FA) = 90°; matrix size = 64 × 64; and voxel size = 3 × 3 × 3 mm. The order of slices was interleaved. After functional image acquisition, T1-weighted high-resolution anatomical images were obtained using a three-dimensional RF-FAST sequence (TR/TE = 12/4.5 ms; FA = 20°; matrix size = 256 × 256; voxel dimension = 1 × 1 × 1 mm).

In fMRI study 2, image scanning was performed using a 3-T scanning system (Magnetom Trio, A Tim System, Siemens, Erlangen, Germany) at the ATR Brain Activity Imaging Center using a 12-channel array coil without acceleration mode. The functional images consisted of 40 consecutive slices parallel to the anterior–posterior commissure plane covering the whole brain. A T2*-weighted gradient-echo echo planar imaging sequence was used with the following parameters: TR/TE = 2500/30 ms; FA = 90°; matrix size = 64 × 64; voxel size = 3 × 3 × 4 mm. The order of slices was ascending. After functional image acquisition, T1-weighted high-resolution anatomical images were obtained using an MP-RAGE sequence (TR = 2,250 ms; TE = 3.06 ms; FA = 9°; matrix size = 256 × 256; voxel size = 1 × 1 × 1 mm).

In the MEG study, anatomical MRI acquisition was performed using the same 3-T scanning system described above with a 12-channel head coil. T1-weighted high-resolution anatomical images were obtained using a MP-RAGE sequence (TR = 2,250 ms; TE = 3.06 ms; field of view = 256 × 256 mm; voxel size = 1 × 1 × 1 mm).

MEG acquisition

MEG data were obtained in an electromagnetic shielded room using a 210-channel whole-head supine position system (PQ1400RM; Yokogawa, Tokyo, Japan). MEG data were sampled at 1,000 Hz through a band pass of 0.05–200 Hz. Vertical and horizontal electrooculograms (EOGs) were recorded simultaneously. Five head-position indicator coils were mounted on the participants' heads to measure the head position within the MEG-sensor system. The coil positions were calibrated electromagnetically before the MEG recordings. The participants' head shape and calibration coil positions were digitized using a three-dimensional laser optical scanner and a stylus marker (FastSCAN Cobra, Polhemus, Vermont, USA).

Analysis: Preprocessing of fMRI data

All analyses of the fMRI data and DCM analyses of the MEG data were performed using the statistical parametric mapping package SPM8 (http://www.fil.ion.ucl.ac.uk/spm) implemented in MATLAB R2012b (Mathworks, Inc., Natick, MA, USA). To preprocess the fMRI data, slice-timing correction was performed to correct for the different times needed to acquire slices in functional images and to increase the robustness of the DCM. To correct for head movements, the functional images were realigned to the first scan as a reference and then realigned again to the mean of the images after the first realignment. Subsequently, the T1 anatomical images were coregistered to the mean of the realigned images. The diffeomorphic anatomical registration using an exponentiated lie algebra (DARTEL) approach was employed to ensure precise spatial normalization. First, the coregistered T1 anatomical images were segmented using a unified segmentation approach (Ashburner and Friston, 2005). Next, the DARTEL algorithm (Ashburner, 2007) was used to create a study-specific template from the gray and white matter images obtained during the segmentation step. The study-specific template was then affine normalized to the Montreal Neurological Institute (MNI) space. Finally, each functional image and T1 anatomical image was normalized spatially to the MNI space by applying the DARTEL warping and affine registration parameters to the study-specific template space and the MNI space. The resulting functional images were resampled to a voxel size of $2 \times 2 \times 2$ and then smoothed using an isotopic Gaussian kernel (6 mm).

Analysis: Preprocessing of MEG data

Continuous MEG data were epoched into 500-ms segments (50-ms pre-stimulus baseline and 450-ms experimental data) for each trial and down-sampled to 200 Hz. The data were initially subjected to independent component analysis (ICA) using the EEGLAB toolbox (http://sccn.ucsd.edu/eeglab/index.html) to reject artifacts. The ICA components were inspected visually, and those representing eye artifacts, heartbeat, or muscle activities were rejected. Threshold-based artifact rejection was also performed. Any epochs containing a gradiometer amplitude $\geq$3,000 fT/cm and an EOG amplitude $\geq$80 mV were rejected as artifacts. An additional small number of epochs containing residual artifacts and trials including artifacts were also excluded after visual inspections. The pre-processed data were then low-pass filtered at 48 Hz, baseline corrected according to the 50-ms pre-stimulus period, and averaged over trials using the conditions for subsequent analyses.

For MEG source reconstruction, an anatomical MRI from each participant was segmented and normalized spatially to the MNI space based on DCM. The inverse of this normalization transformation was then used to warp a canonical cortical mesh in the MNI space to the individual fine-sized cortical mesh (i.e., 20,484 vertices) (Mattout et al., 2007). Next, the MEG sensors were coregistered to the anatomical MRI by matching the positions of three fiducials (nasion and

preauricular points) and head shape. The forward model could then be calculated using a single sphere model.

Analysis: Regional brain activity analysis of fMRI data

To confirm the brain activation and identify the activation foci, random-effects analysis (Holmes and Friston, 1998) was used for the combined data obtained from fMRI studies 1 and 2. First, a single-subject analysis was performed using a general linear model. The task-related blood oxygen level-dependent (BOLD) responses under each condition were modeled using a boxcar function and then convoluted using a canonical hemodynamic response function. A high-pass filter composed of a discrete cosine basis function with a cutoff period of 128 s was used to eliminate the artifactual low-frequency trend. Serial autocorrelation assuming a first-order autoregressive model was estimated from the pooled active voxels with a restricted maximum likelihood (ReML) procedure to whiten the data and the design matrix (Friston et al., 2002). To reduce the motion-related artifacts, the six realignment parameters of the rigid-body transformation estimated in the realignment step were added to the model as nuisance regressors. The dynamic mosaic condition was also added to the data from fMRI study 1 as an effect of no interest.

Planned contrast was then performed to create a contrast image of the main effect of the presentation condition: (dynamic fear + dynamic happiness) vs. (static fear + static happiness) for each participant, which was then entered into two-sample t-tests in the two fMRI studies. The non-sphericity due to uneven variance between the studies was corrected. To assess for commonalities in the main effect of the presentation condition (dynamic vs. static) across fMRI studies, conjunction analysis using a global null hypothesis was performed, which is a convenient method for meta-analyses to combine evidence across studies (Nichols et al., 2005). Significantly activated voxels were identified if they reached the extent threshold of $p < 0.05$ corrected for multiple comparisons, with a height threshold of $p < 0.01$ (uncorrected). Small-volume correction (Worsley et al., 1996) was then conducted for subcortical regions of interest (ROIs), which were defined as 10-mm-radius spheres centered on the activation foci identified in previous studies for the pulvinar (Cotton and Smith, 2007) and amygdala mask, as defined by the automatic anatomical labels (AAL) amygdala mask in the WFU PickAtlas (Maldjian et al., 2003). The other brain regions were analyzed by correcting for the volume of the entire brain. The peak activations were labeled anatomically using Talairach Client (http://www.talairach.org/) after transforming the MNI to Talairach coordinates (icbm2tal; Lancaster et al., 2007) and AAL atlas. We also exploratorily analyzed the effect of emotional category (fear vs. happiness; happiness vs. fear) in the same manner, though a null finding was reported in a previous study (Sato et al., 2012).

Analysis: Connectivity analysis of fMRI data using PPI

PPI analysis is a method used to examining the relationship between activity in different brain areas and their interaction using an experimental treatment (Friston et al., 1997; Gitelman et al., 2003). PPI analysis between the amygdala and neocortical regions was conducted to confirm the results reported in a previous study (Foley et al., 2012). Based on our interest, the amygdala was selected as the seed region.

The amygdala time series was extracted from each participant using the first eigenvariate of 3-mm-radius spheres centered on the participant-specific activation foci, and it was adjusted for confounding factors (realignment parameters and constant term for fMRI studies 1 and 2, and the dynamic mosaic condition for fMRI study 1). Participant-specific maxima that fell within an 8-mm radius around the group maximum were selected using the contrast of the main effect of presentation

(dynamic vs. static), which was masked by the anatomically defined amygdala ROI taken from the Anatomy Toolbox (Eickhoff et al., 2005). Then, the interaction term of the PPI analysis was calculated by multiplying the amygdala activity by the psychological variable (the main effect of presentation condition [dynamic vs. static]) after the amygdala time series was deconvolved using a hemodynamic response function (Gitelman et al., 2003). The convolved regressor for the resulting interaction term, the main effect of the presentation condition (dynamic vs. static), and the amygdala time series were entered into the single-subject general linear model for the PPI analysis. The dynamic mosaic condition and the main effect of emotional category were added as effects of no interest. Other nuisance regressors (realignment parameters and constant terms), high-pass filters, and serial autocorrelations were applied using the same settings described above for regional brain activity analysis.

After the single-subject models for all participants were estimated, contrast images were created for the interaction term and then analyzed using two-sample T-tests to identify commonalities in the PPI between the fMRI studies. Significantly activated voxels were identified as those reaching the extent threshold of $p < 0.05$, corrected for multiple comparisons using a height threshold of $p < 0.01$ (uncorrected). In the same manner, we also conducted exploratory PPI analyses for the main effect of emotional category (fear vs. happiness; happiness vs. fear). However, because we tested the effect of emotional category as a between-subject factor in fMRI study 1 and the PPI analysis does not test modulatory effects for between-subject factors, only the data from fMRI study 2 were used in this analysis.

Analysis: Connectivity analysis of fMRI data using DCM

To explore the effective connectivity between the amygdala and the neocortical regions for the fMRI data, DCM of fMRI (Friston et al., 2003) was conducted using DCM10 in SPM8 software. The DCM allows for modeling of three different types of interactions in a neural network: (1) the driving input, which embodies the influences of an exogenous input on neural states; (2) fixed connections, which represent baseline (i.e., applicable to all experimental conditions) connectivity among neural states; and (3) modulation of intrinsic connections by experimental manipulations.

Based on the results of the regional brain activity analysis and the PPI analysis, together with our interest described in Introduction, we investigated the effect of dynamic presentation, but not that of emotional category. In addition, because the regional brain activity analysis revealed significant activity in some neocortical ROIs only in the right hemisphere and the PPI analysis showed more evident functional couplings in the right hemisphere, we restricted our DCM analysis to the right hemisphere.

To construct the driving and modulatory inputs in the current DCM analysis, we remodeled the single-subject analyses. The design matrix contained the following two experimental factor-specific regressors: the visual input (i.e., all experimental conditions) was the driving input in the DCM, and the dynamic presentation was the modulatory input. The dynamic mosaic condition and the main effect of emotional category were included as effects of no interest. Other nuisance regressors (realignment parameters and constant terms), high-pass filters, and serial autocorrelations were applied at the same settings as described above for the regional brain activity analyses.

To investigate the direction of the amygdala–neocortex functional interaction, seven brain regions in the right hemisphere were selected: the pulvinar (x14, y−30, z0), amygdala (x24, y−8, z−12), primary visual cortex (V1; x18, y−86, z−6), V5/MT (x48, y−60, z0), FG (x44, y−66, z−10), STS (x58, y−38, z14), and IFG (x50, y18, z26). The coordinates of each ROI were defined based on the

results of the regional brain activity analysis at the group level. These ROIs were determined according to the hypothesis described in the Introduction and the results of the PPI analysis, and were restricted to the right hemisphere because some ROIs exhibited significant activities only in the right hemisphere. The ROI time series were extracted for each participant as the first eigenvariate of all voxels within a 3-mm radius around the participant-specific activation foci, and were then adjusted for the effects of no interest and nuisance regressors, high-pass filtered, and corrected for serial correlation. Participant-specific maxima for each region were selected using the following anatomical and functional criteria. The coordinates for the pulvinar were derived from within a 3-mm radius around the group maximum (dynamic vs. static). The coordinates for the amygdala were derived from within the intersection of an 8-mm radius around the group maximum (dynamic vs. static) and the anatomically defined amygdala mask. The coordinates for the V1 were derived from the most significant activation focus in response to dynamic presentation (dynamic vs. rest) within the search region of Brodmann's area (BA) 17, 18. The coordinates for the IFG were derived from within the intersection of a 16-mm radius around the group maximum (dynamic vs. static) and the anatomical mask of BA 44. The coordinates for the FG, V5/MT, and STS were all derived within an 8-mm radius around the group maximum (dynamic vs. static). All anatomical masks were created using the Anatomy Toolbox (Eickhoff et al., 2005).

Next, a hypothesized model (cf. Fig. 3) was constructed for each participant. As a first assumption, the neocortical network, which had a driving input into the V1, and the bi-directional (i.e., forward and backward) intrinsic connections of V1–V5/MT, V1–FG, V5/MT–STS, FG–STS, and STS–IFG were all fixed, and the modulatory effect of dynamic presentation on all intrinsic connections was modeled. This neocortical model was constructed based on the theoretical proposals in the two-pathway model (Oram and Perrett, 1996) and the mirror neuron system model (Kana et al., 2011) for processing dynamic social signals. This neocortical network model was validated in a previous DCM using MEG data (Sato et al., 2015), and a similar (partially simplified) model was also validated using fMRI data (Sato et al., 2012). As a second assumption, the subcortical network, which had the driving input into the pulvinar, and the forward intrinsic connection of the pulvinar–amygdala were fixed, and the modulatory effect of dynamic presentation on this intrinsic connection was predicted. This subcortical network was constructed based on theoretical (e.g., Vuilleumier and Pourtois, 2007) and empirical (e.g., Morris et al., 1999) evidence for the processing of emotional facial expressions. Although the studies posited that the superior colliculus sends input to the pulvinar, we did not include the superior colliculus in the current model because this region was located adjacent to the pulvinar, making it difficult to dissociate using the defined ROI selection method, and also because the analyses of regional brain activity and effective connectivity did not reveal the involvement of this region, probably due to a lack of spatial resolution and signal-to-noise ratio. As a third assumption, we tested the connectivity between the amygdala and the V5/MT, FG, STS, and IFG neocortical regions. This was because the PPI analysis revealed a functional interaction between the amygdala and these regions, which was consistent with the results of a previous study (Foley et al., 2012).

Based on the direction of the intrinsic connections and the locations of modulatory effects, we then constructed the following five models (Figure 3): (1) the "directional connectivity from the amygdala" model, which had intrinsic and modulatory connections from the amygdala to the neocortex; (2) the "directional connectivity to the amygdala" model, which had intrinsic and modulatory connections from the neocortex to the amygdala; (3) the "bi-directional" model, which had bi-directional intrinsic and modulatory connections between the amygdala and neocortex; (4) the "directional connectivity from the amygdala (only modulatory)" model, which had bi-directional intrinsic and one-directional modulatory connections from the amygdala to the neocortex; and (5) the

"directional connectivity to the amygdala (only modulatory)" model, which had bi-directional intrinsic and one-directional modulatory connections from the neocortex to the amygdala.

To examine the direction of amygdala–neocortex connectivity and its network structure, we conducted separate analyses in both fMRI studies and tested the most appropriate model using a random-effects Bayesian model selection (BMS) (Stephan et al., 2009). We used the exceedance probabilities as the evaluation measures based on the belief that a particular model was more likely to be accurate than any other model given the group data (cf. Liu et al., 2010; Seghier et al., 2011).

Analysis: Connectivity analysis of MEG data using DCM

DCM analysis of the MEG data was also performed using DCM for the event-related potential (ERP) modeling of the electrophysiological data (David et al., 2006). This is a source reconstruction technique that allows spatial electromagnetic forward models and neurobiologically informed temporal forward models to be inverted to describe the connectivity patterns among sources. A detailed description of the theory and practical implementation of the use of DCM for ERP was provided previously (David et al., 2006; Litvak, et al., 2011). Here, only information relevant to the current analysis is described briefly.

To identify the optimal amygdala–neocortex connectivity pattern in the electrophysiological activity, the same models were compared with those used to analyze the fMRI studies. Each source was modeled using a single equivalent current dipole (ECD) with prior fixed locations and a variance of 4 mm. ECDs were placed over the center coordinates of the fMRI group analysis described above, except that the pulvinar was modeled as a hidden source to allow subcortical activity such as that of the thalamus to be modeled without contributing to the measured MEG signals. This method was used previously to examine subcortical–cortical connectivity during auditory language processing (David et al., 2011), emotional face processing (Garrido et al., 2012), and the steady-state EEG response (Boly et al., 2012). The onset time parameter for the driving input was set at 80 ms. Random-effects BMS was then applied to define the most plausible model (Stephan et al., 2009). To specify the time-dependent directional change in the amygdala-neocortex connectivity, the models were compared using an increasing time-window approach (Garrido et al., 2007; Garrido et al., 2012). To simplify the model comparisons, the "directional connectivity from the amygdala" and the "directional connectivity to the amygdala" models were compared based on the results of the above DCM because these models had comparable complexity with the target model. Random-effects BMS was performed using eight data segments with lengths increasing from 100 to 450 ms in 50-ms increments after the stimulus onset.

Results

Regional brain activity in fMRI data

When the brain activity in response to dynamic facial expressions was compared with that in response to static expressions for the data using the conjunction analysis from fMRI studies 1 and 2, broad posterior regions in both hemispheres, including the V5/MT, FG, STS, and IFG activation foci in the right hemisphere, were significantly activated (Table 1; Fig. 1). Significant activation was also observed in the amygdala and pulvinar in both hemispheres after a small volume correction. When the effect of emotional category was exploratorily tested in the same manner, no significant activation was detected.

PPI analysis of fMRI data

The conjunction analysis for the PPI of fMRI studies 1 and 2 revealed that, when the right amygdala was selected as the seed region, broad neocortical regions in the right hemispheres, including the activation foci of the STS and IFG, were correlated more significantly with the activity in the amygdala during the observation of dynamic facial expressions compared with static facial expressions (Table 2; Fig. 2). With a more liberal extent threshold ($p < 0.01$, uncorrected), activation exhibiting increased correlations with the right amygdala activity during dynamic than during static facial expressions was found in the V5/MT and FG in the right hemisphere. When the left amygdala was selected as the seed region, the neocortical regions in the right hemispheres showed a similar but less evident pattern. Specifically, there was no significant cluster with the predefined threshold; with a liberal extent threshold ($p < 0.01$, uncorrected), the V5/MT and IFG in the right hemisphere were detected (x34, y-60, z-10; $Z = 3.85$; cluster size = 364 voxels; x42, y-2, z30; $Z = 4.13$; cluster size = 237 voxels). The STS and FG in the right hemisphere showed non-significant trends. The PPI analysis for the effect of emotional category showed no significant clusters with the predefined threshold. With a liberal extent threshold ($p < 0.01$, uncorrected), a cluster was detected around the left middle occipital gyrus (x-22, y-88, z22; $Z = 3.34$; cluster size = 530 voxels) for a higher correlation with right amygdala activity for fearful than happy expressions; some other visual cortices, including the bilateral FG, showed non-significant trends of the same correlation changes with amygdala activity in the same hemispheres.

DCM analysis of fMRI data

DCM analyses were conducted using the data from fMRI study 1 to test the network models with different intrinsic and modulatory connectivity between the amygdala and neocortical regions (Fig. 3). Based on the above findings, together with our interest, we analyzed the effect of dynamic presentation, but not that of emotional category. In addition, we restricted our DCM analysis to the right hemisphere. The exceedance probability of the random-effects BMS indicated that the "directional connectivity from the amygdala" model was the most likely (Fig. 4). DCM analyses of the data from fMRI study 2 supported the same model (Fig. 4).

DCM analysis of MEG data

DCM and random-effects BMS were applied to the MEG data. Consistent with the fMRI analyses, the BMS exceedance probability was highest for the "directional connectivity from the amygdala" model (Fig. 4).

Increasing time-window analysis of DCM using MEG data

The increasing time-window analysis of DCM was performed using the MEG data to elucidate the time-dependent directional change in the amygdala–neocortex connectivity. The "directional connectivity from the amygdala" and "directional connectivity to the amygdala" models were compared over post-stimulus time windows of 100–500 ms in 50-ms increments. The random-effects BMS showed that the "directional connectivity from the amygdala" model accounted for the data

better than did the “directional connectivity to the amygdala” model at 200–250 ms and 300–500 ms (Fig. 5).

Discussion

The results of the current PPI analysis of the fMRI data showed that the amygdala and neocortical regions, including the V5, FG, STS, and IFG, functionally interacted during the observation of dynamic facial expressions of emotion. These results are consistent with those reported in a previous fMRI study (Foley et al., 2012). These data suggest an interaction between emotional and perceptual/cognitive/motor processing during dynamic facial expression processing.

More importantly, the results of DCM for the fMRI data revealed that the direction of this amygdala-neocortex interaction was from the amygdala to the neocortex. The results of two independent fMRI studies consistently supported a model that had intrinsic and modulatory connections from the amygdala to the neocortex. This is consistent with the hypothesis that the amygdala would be activated more rapidly than the neocortex would, and it would then modulate neocortical activity during the processing of emotional facial expressions (e.g., Vuilleumier and Pourtois, 2007). However, empirical evidence to support this proposal has been lacking. Although a previous PPI analysis showed a functional interaction between the amygdala and neocortex during the processing of dynamic facial expressions (Foley et al., 2012), its direction was unclear because PPI cannot provide information regarding the direction of functional interactions (Friston, 2011). To our knowledge, this is the first evidence that the amygdala modulates neocortical activity during the processing of dynamic facial expressions of emotion.

The DCM results using MEG data also supported a model of functional interaction from the amygdala to the neocortical regions during the observation of dynamic facial expressions. Because MEG detects electromagnetic signals of neuronal activity, which is a more direct measure than the BOLD signal detected using fMRI, and has higher temporal resolution, at the millisecond level relative to the few-second level of fMRI (Dale and Halgren, 2001), the convergence of the two sets of results increases the reliability of the conclusions.

These results showing neural interaction from the amygdala to the neocortex have implications for information processing of dynamic facial expressions. Ample evidence from neuroimaging and neuropsychological studies suggests that the amygdala is involved in emotional processing for facial expressions (Calder et al., 2001). For example, previous fMRI studies showed that the activity in the amygdala corresponded to subjective emotional arousal/intensity (Sato et al., 2004, 2010). The evidence also suggests that neocortical regions play a crucial role in processing other information, such as the visual analysis of invariant aspects of faces and/or the subjective perception of faces in the FG (Haxby et al., 2000), the visual analysis of dynamic aspects of faces and the recognition of the inner states of others in the STS (Allison et al., 2000; Frith, 2001), and motor mimicry in the IFG (Iacoboni, 2005). Together with these data, the current results suggest that the emotional processing related to amygdala activity modulates the perceptual, cognitive, and motor processing of the neocortical regions during the observation of dynamic facial expressions. This is consistent with behavioral studies. For example, a previous behavioral study reported that the representational

momentum perception (illusory enhancement of perception) for dynamic facial expressions differed depending on the emotional intensity of the facial expressions (Yoshikawa and Sato, 2008), and the researchers speculated that the emotional message modulates the perception of dynamic facial expressions. Another study (Cunningham and Wallraven, 2009) showed that the emotional recognition of dynamic facial expressions was reduced when the stimuli were presented backward (i.e., with weaker emotional arousal compared with forward presentations; Sato et al., 2010). A study that recorded participants' facial muscle reactions during the observation of emotional facial expressions and manipulated their emotions found that the congruent facial reactions in response to stimulus facial expressions were modulated by the participants' own emotional states (Moody et al., 2007). Hess and Fischer (2013) reviewed literature related to facial mimicry, and proposed that emotional information influences facial motor reactions in response to emotional facial expressions. Together with these data, the current results suggest that the functional interaction from the amygdala to the neocortical regions may represent a neural mechanism that serves to implement the influence of emotion on perceptual, cognitive, and motor responses to dynamic facial expressions.

Furthermore, the current result of the increasing time-window DCM specified the times at which the functional interactions from the amygdala to the neocortex were accomplished. The model based on the influence of the amygdala on the neocortex accounted for the data after 200 ms better than did the reverse model. If this is interpreted to mean that amygdala activity reflects the emotional processing of facial expressions, this time frame is consistent with the results of several scalp EEG studies investigating the impact of emotion on neocortical activity. These studies showed that a greater negative deflection was elicited at ~200–400 ms in the posterior neocortex in response to emotional facial expressions (e.g., Sato et al., 2001; Balconi and Pozzoli, 2003) and emotional scenes (e.g., Junghoefer et al., 2001; Schupp et al., 2003) compared with neutral ones. A recent study showed that the amplitude of this component in response to emotional facial expressions was related to increased emotional arousal and enhanced perception of facial expression stimuli (Sawada et al., 2014). Together with these data, the current results suggest that the functional interactions from the amygdala to the neocortex are implemented after 200 ms and reflect the effects of emotion on perceptual/cognitive/motor processing during the observation of dynamic facial expressions.

The regional brain activity and PPI analyses of the fMRI data showed that neocortical activation and amygdala–neocortex functional interactions during dynamic facial expression processing was more evident in the right than in the left hemisphere. The right-hemispheric activation dominance in response to dynamic facial expressions is consistent with the results of several other neuroimaging studies (e.g., De Winter et al., 2015). The right-hemispheric dominance for the processing of facial expressions is also in line with evidence from patients with brain damage (Abbott et al., 2013; Yuvaraj et al., 2013). Because a previous PPI study (Foley et al., 2012) analyzed amygdala–neocortex functional interaction for dynamic facial expression processing only using the seed in the right amygdala, this study provides the first evidence that the amygdala–neocortex functional interaction is more evident in the right, compared with the left, hemisphere. Our data suggest that the right hemisphere is dominant in the processing of facial expressions, at least partially because its amygdala–neocortex interaction is more efficient than that in the left hemisphere.

The PPI analysis of the fMRI data in terms of the effect of emotional category showed that the amygdala modulated the early visual cortices during the processing of fearful vs. happy expressions. This result is consistent with the finding of a previous study (Morris et al., 1998). However, the modulatory effect of emotional category was not evident compared with that of the presentation condition. This result appears to be in line with the results of several neuroimaging studies showing that the amygdala was comparably active in response to facial expressions of positive and negative emotional categories (e.g., van der Gaag et al., 2007; for a review, see Sergerie et al., 2008). Together with these data, we speculate that amygdala activation and its modulation of the neocortex may not differ noticeably across emotional categories. However, it must be noted that the data set for the analysis of the emotional category effect was smaller than that for the presentation condition because of the experimental design. Further studies are needed to define changes in the neocortical modulatory effect of the amygdala depending on emotional categories.

Some limitations of the present study should be acknowledged. First, because we analyzed the fMRI data from different magnetic field strengths, such differences may have affected our results. There are well-known advantages and disadvantages of 1.5T and 3T MRI scanners (Krasnow et al., 2003; Preston et al., 2004). Specifically, 3T MRI is more beneficial than 1.5T for fMRI experiments, because an increase in magnetic field strength yields a greater increase in BOLD contrasts during functional activation. On the other hand, susceptibility artifacts consisting of signal dropouts and image distortions are more pronounced at 3T than at 1.5T field strengths. For regional brain activity analyses, a previous technical study reported that the mixing of 1.5T and 3T fMRI data can compensate for these drawbacks by increasing statistical power and reducing the incorrect detection of activation (Han and Talavage, 2011). Hence, we conducted the conjunction analysis in a meta-analysis fashion (Nichols et al., 2005), which provided more robust and accurate evidence compared with the separate evaluation of 1.5T and 3T fMRI data. In fact, the main effect of presentation condition was successfully replicated. For the PPI analyses, it is plausible that BOLD signals are affected in both an advantageous and disadvantageous manner affected by magnetic field strengths, similar to regional brain activity analysis. Therefore, we again conducted the conjunction analysis in a meta-analysis fashion (Nichols et al., 2005) to test the effect of presentation condition. For the DCM analysis, we reasoned that differences in field strengths would not greatly affect the results, because (1) DCM separately models the neural state model and the hemodynamic state model and (2) differential hemodynamic responses from different field strengths are accommodated by free biophysical parameters in the hemodynamic model (Stephan et al., 2007). However, the precise effects of different field strengths on the functional and effective connectivity analyses remain unknown and must be explored further.

Second, although DCM and ERP modeling DCM were used to analyze the fMRI data and MEG data, respectively, the best method to analyze the connectivity among brain regions effectively remains controversial. For example, a study highlighted a limitation of the nonlinear relationship in DCM, and proposed an alternative method that could analyze nonlinear effective connectivity among brain regions efficiently (Liu and Aviyente, 2012). Regarding the analysis of the MEG data, a previous study proposed that consideration of the frequency domain might be useful to analyze the

causal relationships among electric neural interactions (Chen et al., 2008). Future studies applying different methods would be useful in further analyzing the models tested in the present study.

In conclusion, the current DCM analysis of fMRI and MEG data revealed that the direction of functional interaction during dynamic facial expressions was from the amygdala to the neocortex. The analysis of MEG data further confirmed that this was accomplished at 200 ms from the stimulus onset. These data suggest that emotional processing in the amygdala rapidly modulates neocortical processing, including perception, recognition, and motor mimicry, during the observation of dynamic facial expressions of emotion.

Funding

This study was supported by funds from the Japan Society for the Promotion of Science Funding Program for Next Generation World-Leading Researchers (LZ008).

Notes

Conflict of interest: None declared.

References

Abbott JD, Cumming G, Fidler F, Lindell AK. 2013. The perception of positive and negative facial expressions in unilateral brain-damaged patients: A meta-analysis. Laterality. 18: 437–459.

Adolphs R. 2001. The neurobiology of social cognition. Curr Opin Neurobiol. 11: 231–239.

Allison T, Puce A, McCarthy G. 2000. Social perception from visual cues: Role of the STS region. Trends Cogn Sci. 4: 267–278.

Amaral DG, Price JL. 1984. Amygdalo-cortical projections in the monkey (Macaca fascicularis). J Comp Neurol. 230: 465–496.

Amaral DG, Price JL, Pitkanen A, Carmichael ST. 1992. Anatomical organization of the primate amygdaloid complex. In: Aggleton JP, editor. The amygdala: Neurobiological aspects of emotion, memory, and mental dysfunction. New York: Wiley-Liss.

Arsalidou M, Morris D, Taylor MJ. 2011. Converging evidence for the advantage of dynamic facial expressions. Brain Topogr. 24: 149–163.

Ashburner J. 2007. A fast diffeomorphic image registration algorithm. Neuroimage. 38: 95–113.

Ashburner J, Friston KJ. 2005. Unified segmentation. Neuroimage. 26: 839–851.

Avendano C, Price JL, Amaral DG. 1983. Evidence for an amygdaloid projection to premotor cortex but not to motor cortex in the monkey. Brain Res. 264:111–117.

Balconi M, Pozzoli U. 2003. Face-selective processing and the effect of pleasant and unpleasant emotional expressions on ERP correlates. Int J Psychophysiol. 49: 67–74.

Boly M, Moran R, Murphy M, Boveroux P, Bruno MA, Noirhomme Q, Ledoux D, Bonhomme V, Brichant JF, Tononi G, Laureys S, Friston K. 2012. Connectivity changes underlying spectral EEG changes during propofol-induced loss of consciousness. J Neurosci. 32: 7082–7090.

Bould E, Morris N, Wink B. 2008. Recognising subtle emotional expressions: The role of facial movements. Cogn Emot. 22: 1569–1587.

Calder AJ, Lawrence AD, Young AW. 2001. Neuropsychology of fear and loathing. Nat Rev Neurosci. 2: 352–363.

Catani M, Jones DK, Donato R, Ffytche DH. 2003. Occipito-temporal connections in the human brain. Brain. 126: 2093–2107.

Chen CC, Kiebel SJ, Friston KJ. 2008. Dynamic causal modelling of induced responses. Neuroimage. 41: 1293–1312.

Cotton PL, Smith AT. 2007. Contralateral visual hemifield representations in the human pulvinar nucleus. J. Neurophysiol. 98: 1600–1609.

Cunningham DW, Wallraven C. 2009. Dynamic information for the recognition of conversational expressions. J Vis. 9: 7.

Dale AM, Halgren E. 2001. Spatiotemporal mapping of brain activity by integration of multiple imaging modalities. Curr Opin Neurobiol. 11: 202–208.

Darwin C. 1872. The expression of the emotions in man and animals. London: UK. Murray.

David O, Kiebel SJ, Harrison LM, Mattout J, Kilner JM, Friston KJ. 2006. Dynamic causal modeling of evoked responses in EEG and MEG. Neuroimage. 30: 1255–1272.

David O, Maess B, Eckstein K, Friederici AD. 2011. Dynamic causal modeling of subcortical connectivity of language. J Neurosci. 31: 2712–2717.

Day-Brown JD, Wei H, Chomsung RD, Petry HM, Bickford ME. 2010. Pulvinar projections to the striatum and amygdala in the tree shrew. Front Neuroanat. 4: 143.

De Winter FL, Zhu Q, Van den Stock J, Nelissen K, Peeters R, de Gelder B, Vanduffel W, Vandenbulcke M. 2015. Lateralization for dynamic facial expressions in human superior temporal sulcus. Neuroimage. 106: 340–352.

Eickhoff SB, Stephan KE, Mohlberg H, Grefkes C, Fink GR, Amunts K, Zilles K. 2005. A new SPM toolbox for combining probabilistic cytoarchitectonic maps and functional imaging data. Neuroimage. 25: 1325–1335.

Ekman P, Friesen W V. 1976. Pictures of Facial Affect. Palo Alto: Consulting Psychologist.

Foley E, Rippon G, Thai NJ, Longe O, Senior C.2012. Dynamic facial expressions evoke distinct activation in the face perception network: A connectivity analysis study. J Cogn Neurosci. 24: 507–520.

Friston KJ. 2011. Functional and effective connectivity: A review. Brain Connect. 1: 13–36.

Friston KJ, Buechel C, Fink GR, Morris J, Rolls E, Dolan RJ. 1997. Psychophysiological and modulatory interactions in neuroimaging. Neuroimage. 6: 218–229.

Friston KJ, Glaser DE, Henson RN, Kiebel S, Phillips C, Ashburner J. 2002. Classical and Bayesian inference in neuroimaging: Applications. Neuroimage. 16: 484–512.

Friston KJ, Harrison L, Penny W. 2003. Dynamic causal modelling. Neuroimage. 19: 1273–1302.

Frith U. 2001. Mind blindness and the brain in autism. Neuron. 32: 969–979.

Garrido MI, Barnes GR, Sahani M, Dolan RJ. 2012. Functional evidence for a dual route to amygdala. Curr. Biol. 22: 129–134.

Garrido MI, Kilner JM, Kiebel SJ, Friston KJ. 2007. Evoked brain responses are generated by feedback loops. Proc Natl Acad Sci U S A. 104: 20961–20966.

Gitelman DR, Penny WD, Ashburner J, Friston KJ. 2003. Modeling regional and psychophysiologic interactions in fMRI: The importance of hemodynamic deconvolution. Neuroimage. 19: 200–207.

Grèzes J, Valabregue R, Gholipour B, Chevallier C. 2014. A direct amygdala-motor pathway for emotional displays to influence action: A diffusion tensor imaging study. Hum Brain Mapp. 35: 5974–5983.

Grèzes J, Wicker B, Berthoz S, de Gelder B. 2009. A failure to grasp the affective meaning of actions in autism spectrum disorder subjects. Neuropsychologia. 47: 1816–1825.

Han K, Talavage TM. 2011. Effects of combining field strengths on auditory functional MRI group analysis: 1.5T and 3T. J Magn Reson Imaging. 34: 1480–1488.

Haxby JV, Hoffman EA, Gobbini MI. 2000. The distributed human neural system for face perception. Trends Cogn Sci. 4: 223–233.

Hess U, Fischer A. 2013. Emotional mimicry as social regulation. Pers Soc Psychol Rev. 24:142–157.

Holmes AP, Friston KJ. 1998. Generalisability, random effects and population inference. Neuroimage. 7: S754.

Iacoboni M. 2005. Neural mechanisms of imitation. Curr Opin Neurobiol. 15: 632–637.

Junghoefer M, Bradley MM, Ebert T, Lang P. 2001. Fleeting images: A new look at early emotion discrimination. Psychophysiology. 38: 175–178.

Kana RK, Wadsworth HM, Travers BG. 2011. A systems level analysis of the mirror neuron hypothesis and imitation impairments in autism spectrum disorders. Neurosci Biobehav Rev. 35: 894–902.

Krasnow B, Tamm L, Greicius MD, Yang TT, Glover GH, Reiss AL, Menon V. 2003. Comparison of fMRI activation at 3 and 1.5 T during perceptual, cognitive, and affective processing. Neuroimage. 18: 813–826.

LaBar KS, Crupain MJ, Voyvodic JT, McCarthy G. 2003. Dynamic perception of facial affect and identity in the human brain. Cereb Cortex. 13: 1023–1033.

Lancaster JL, Tordesillas-Gutierrez D, Martinez M, Salinas F, Evans A, Zilles K, Mazziotta JC, Fox PT. 2007. Bias between MNI and Talairach coordinates analyzed using the ICBM-152 brain template. Hum. Brain Mapp. 28: 1194–1205.

Lazarus RS. 1982. Thoughts on the relations between emotion and cognition. Am Psychol. 37: 1019–1024.

Litvak V, Mattout J, Kiebel S, Phillips C, Henson R, Kilner J, Barnes G, Oostenveld R, Daunizeau J, Flandin G, Penny W, Friston K. 2011. EEG and MEG data analysis in SPM8. Comput. Intell. Neurosci. 2011: 852961.

Liu L, Vira A, Friedman E, Minas J, Bolger D, Bitan T, Booth J. 2010. Children with reading disability show brain differences in effective connectivity for visual, but not auditory word comprehension. PLoS One. 5: e13492.

Liu Y, Aviyente S. 2012. Quantification of effective connectivity in the brain using a measure of directed information. Comput Math Methods Med. 2012: 635103.

Maldjian JA, Laurienti PJ, Kraft RA, Burdette JH. 2003. An automated method for neuroanatomic and cytoarchitectonic atlas-based interrogation of fMRI data sets. Neuroimage. 19: 1233–1239.

Mattout J, Henson RN, Friston KJ. 2007. Canonical source reconstruction for MEG. Comput Intell Neurosci. 2007: 67613.

Mehrabian A. 1971. Nonverbal communication. In: Cole JK, editor. Nebraska Symposium on Motivation 1971. Lincoln: University of Nebraska Press. pp. 107–161.

Moody EJ, Mcintosh DN, Mann LJ, Weisser KR. 2007. More than mere mimicry? The influence of emotion on rapid facial reactions to faces. Emotion. 7: 447–457.

Morris JS, Friston KJ, Buchel C, Frith CD, Young AW, Calder AJ, Dolan RJ. 1998. A neuromodulatory role for the human amygdala in processing emotional facial expressions. Brain. 121: 47–57.

Morris JS, Öhman A, Dolan RJ. 1999. A subcortical pathway to the right amygdala mediating "unseen" fear. Proc Natl Acad Sci U S A. 96: 1680–1685.

Nichols T, Brett M, Andersson J, Wager T, Poline J-B. 2005. Valid conjunction inference with the minimum statistic. Neuroimage. 25: 653–660.

Oram MW, Perrett DI. 1996. Integration of form and motion in the anterior superior temporal polysensory area (STPa) of the macaque monkey. J Neurophysiol. 76: 109–126.

Preston AR, Thomason ME, Ochsner KN, Cooper JC, Glover GH. 2004. Comparison of spiral-in/out and spiral-out BOLD fMRI at 1.5 and 3 T. Neuroimage. 21: 291–301.

Rafal RD, Koller K, Bultitude JH, Mullins P, Ward R, Mitchell AS, Bell AH. 2015. Connectivity between the superior colliculus and the amygdala in humans and macaque monkeys: Virtual dissection with probabilistic DTI tractography. J Neurophysiol. 114: 1947–1962.

Sato W, Kochiyama T, Uono S, Matsuda K, Usui K, Inoue Y, Toichi M. 2011. Rapid amygdala gamma oscillations in response to fearful facial expressions. Neuropsychologia. 49: 612–617.

Sato W, Kochiyama T, Uono S, Matsuda K, Usui K, Inoue Y, Toichi M. 2013. Rapid and multiple-stage activation of the human amygdala for processing facial signals. Commun Integr Biol. 6: e24562.

Sato W, Kochiyama T, Uono S. 2015. Spatiotemporal neural network dynamics for the processing of dynamic facial expressions. Sci Rep. 5: 12432.

Sato W, Kochiyama T, Yoshikawa S. 2010. Amygdala activity in response to forward versus backward dynamic facial expressions. Brain Res. 1315: 92–99.

Sato W, Kochiyama T, Yoshikawa S, Matsumura M. 2001. Emotional expression boosts early visual processing of the face: ERP recording and its decomposition by independent component analysis. Neuroreport. 12: 709–714.

Sato W, Kochiyama T, Yoshikawa S, Naito E, Matsumura M. 2004. Enhanced neural activity in response to dynamic facial expressions of emotion: An fMRI study. Brain Res Cogn Brain Res. 20: 81–91.

Sato W, Kubota T, Toichi M. 2014. Enhanced subliminal emotional responses to dynamic facial expressions. Front Psychol. 5: 994.

Sato W, Toichi M, Uono S, Kochiyama T. 2012. Impaired social brain network for processing dynamic facial expressions in autism spectrum disorders. BMC Neurosci. 13: 99.

Sato W, Yoshikawa S. 2004. The dynamic aspects of emotional facial expressions. Cogn Emot. 18: 701–710.

Sato W, Yoshikawa S. 2007a. Spontaneous facial mimicry in response to dynamic facial expressions. Cognition. 104: 1–18.

Sato W, Yoshikawa S. 2007b. Enhanced experience of emotional arousal in response to dynamic facial expressions. J Nonverbal Behav. 31: 119–135.

Sawada R, Sato W, Uono S, Kochiyama T, Toichi M. 2014. Electrophysiological correlates of detecting emotional facial expressions. Brain Res. 1560: 60–72.

Schupp HT, Junghofer M, Weike AI, Hamm AO. 2003. Emotional facilitation of sensory processing in the visual cortex. Psychol Sci. 14: 7–13.

Seghier ML, Josse G, Leff AP, Price CJ. 2011. Lateralization is predicted by reduced coupling from the left to right prefrontal cortex during semantic decisions on written words. Cereb Cortex. 21: 1519–1531.

Sergerie K, Chochol C, Armony JL. 2008. The role of the amygdala in emotional processing: A quantitative meta-analysis of functional neuroimaging studies. Neurosci. Biobehav. Rev. 32: 811–830.

Stephan KE, Penny WD, Daunizeau J, Moran RJ, Friston KJ. 2009. Bayesian model selection for group studies. Neuroimage. 46: 1004–1017.

Stephan KE, Weiskopf N, Drysdale PM, Robinson PA, Friston KJ. 2007. Comparing hemodynamic models with DCM. Neuroimage. 38: 387–401.

Steriade M, Amzica F, Nunez A. 1993. Cholinergic and noradrenergic modulation of the slow (approximately 0.3 Hz) oscillation in neocortical cells. J Neurophysiol. 70: 1385–1400.

Tamietto M, Pullens P, de Gelder B, Weiskrantz L, Goebel R. 2012. Subcortical connections to human amygdala and changes following destruction of the visual cortex. Curr Biol. 22: 1449–1455.

Tsuchiya N, Kawasaki H, Oya H, Howard MA3, Adolphs R. 2008. Decoding face information in time, frequency and space from direct intracranial recordings of the human brain. PLoS One. 3: e3892.

van der Gaag C, Minderaa RB, Keysers C. 2007. The BOLD signal in the amygdala does not differentiate between dynamic facial expressions. Soc Cogn Affect Neurosci. 2: 93–103.

Vuilleumier P, Pourtois G. 2007. Distributed and interactive brain mechanisms during emotion face perception: evidence from functional neuroimaging. Neuropsychologia. 45: 174–194.

Worsley KJ, Marrett S, Neelin P, Vandal AC, Friston KJ, Evans AC. 1996. A unified statistical approach for determining significant signals in images of cerebral activation. Hum Brain Mapp. 4: 58–73.

Yoshikawa S, Sato W. 2008. Dynamic facial expressions of emotion induce representational momentum. Cogn Affect Behav Neurosci. 8: 25–31.

Yuvaraj R, Murugappan M, Norlinah MI, Sundaraj K, Khairiyah M. 2013. Review of emotion recognition in stroke patients. Dement Geriatr Cogn Disord. 36: 179–196.

Zajonc RB. 1980. Feeling and thinking: Preferences need no inferences. Am Psychol. 35: 151–175.

Table 1. The brain regions that exhibited significant activation in response to dynamic vs. static facial expression conditions in the conjunction of fMRI studies 1 and 2.

Brain region	BA	Coordinates			Z-value	Cluster size
		x	y	z		(voxels)
R. Middle Frontal Gyrus	6	48	6	40	6.40	6026
R. Inferior Frontal Gyrus	9	48	18	26	4.46	
L. Inferior Temporal Gyrus	37	-46	-68	4	8.13	7762
L. Cuneus	17	-20	-88	12	5.60	
L. Inferior Parietal Lobule	40	-58	-38	22	4.00	
L. Superior Temporal Gyrus	22	-56	-44	14	4.00	
R. Middle Temporal Gyrus	37	48	-60	0	8.13	1912
R. Fusiform Gyrus	37	44	-66	-10	8.13	
R. Inferior Occipital Gyrus	19	40	-74	0	8.13	
R. Precuneus	31	26	-80	30	7.03	
R. Inferior Parietal Lobule	40	56	-24	32	6.53	
R. Superior Temporal Gyrus	13	58	-38	14	5.52	
L. Amygdala		-28	-6	-12	5.48	52*
R. Amygdala		24	-8	-12	3.83	13*
L. Pulvinar		-10	-26	-2	2.52	20*
R. Pulvinar		14	-30	0	2.91	31*

$p < 0.05$ cluster level corrected; * using small volume correction.

Table 2. The brain regions that exhibited significant psychophysiological interaction with the right amygdala during dynamic facial expression conditions in the conjunction of fMRI studies 1 and 2.

Brain region	BA	Coordinates			Z-value	Cluster size
		x	y	z		(voxels)
R. Middle Frontal Gyrus	6	54	10	38	4.72	6026
R. Superior Temporal Gyrus	22	62	-42	14	4.02	
R. Precentral Gyrus	6	52	8	46	3.93	
R. Inferior Parietal Lobule	40	60	-36	26	3.12	
R. Inferior Frontal Gyrus	9	52	12	18	2.74	
R. Inferior Temporal Gyrus	37	48	-68	-2	4.51	330^{+}
R. Fusiform Gyrus	37	40	-48	-12	3.31	
R. Lingual Gyrus	18	34	-74	-4	3.11	
R. Middle Occipital Gyrus	19	48	-76	8	2.61	

$p < 0.05$ cluster level corrected; + Uncorrected liberal extent threshold of $p < 0.01$.

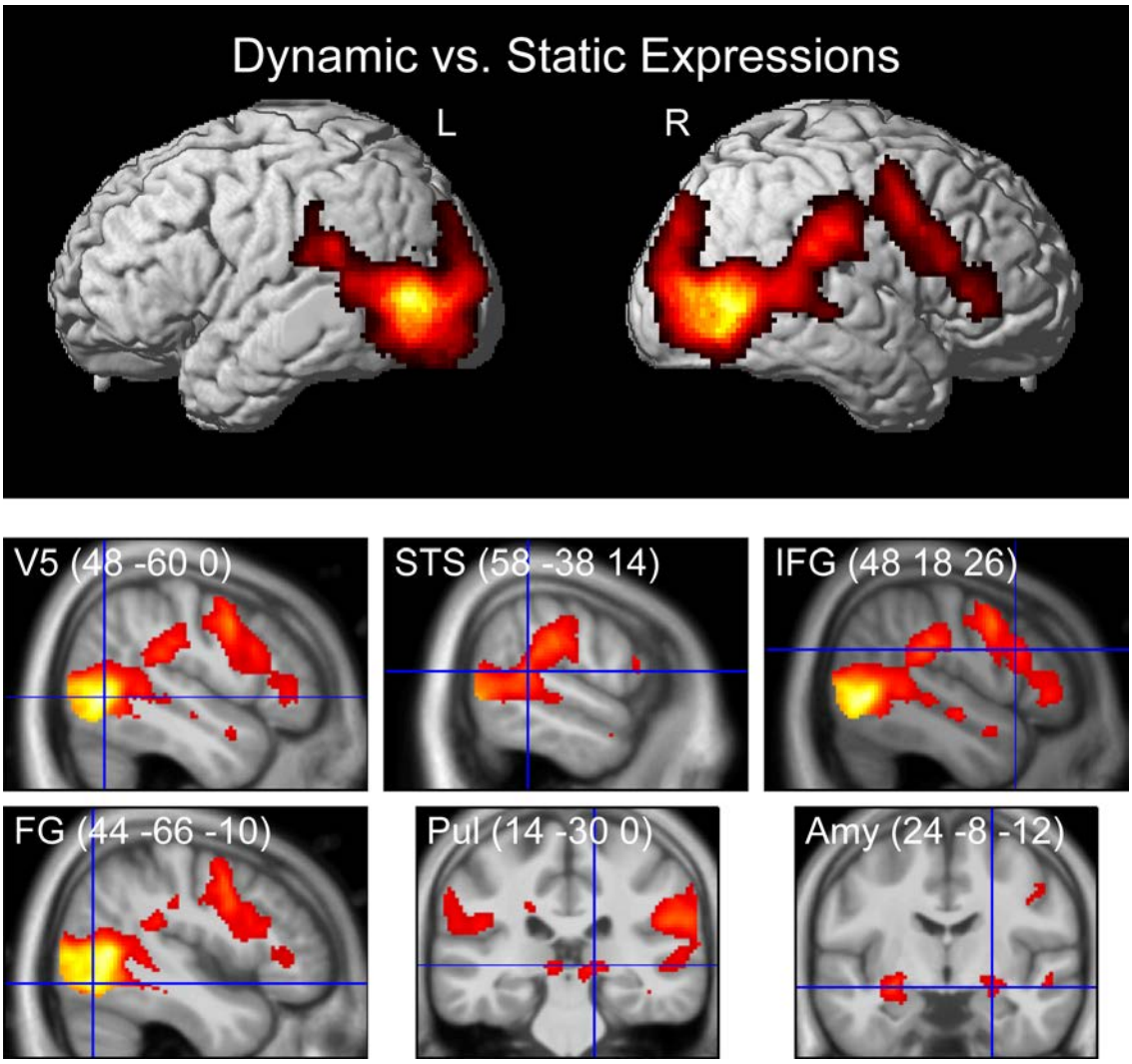

Figure 1.

Statistical parametric maps of the conjunction analysis showing significant activation in response to dynamic facial expressions compared with static expressions across functional magnetic resonance imaging studies. The areas of activation are rendered on spatially normalized brains (upper panel). The regions of interest and the center coordinates were selected for dynamic causal modeling (lower panel). L = left; R = right; V5 = V5/middle temporal area; FG = fusiform gyrus; STS = superior temporal sulcus; IFG = inferior frontal gyrus; Amy = amygdala; Pul = pulvinar.

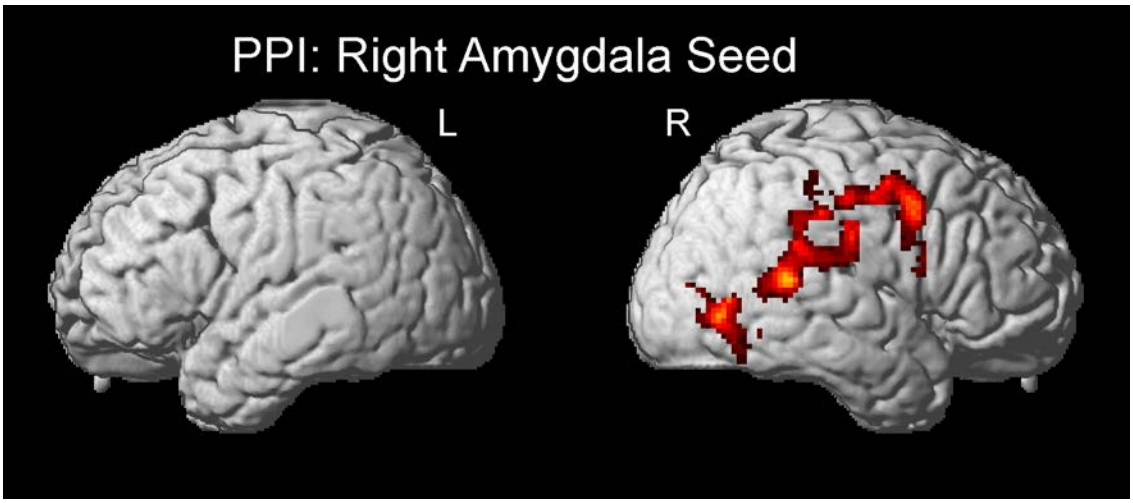

Figure 2.

Statistical parametric maps of the conjunction analysis for psychophysiological interaction (PPI) showing significant connectivity with the right amygdala in response to dynamic vs. static facial expressions in both functional magnetic resonance imaging studies. The result is rendered on spatially normalized brains. Note that the extent threshold is set at $p < 0.01$ and is uncorrected for display purposes. L = left; R = right.

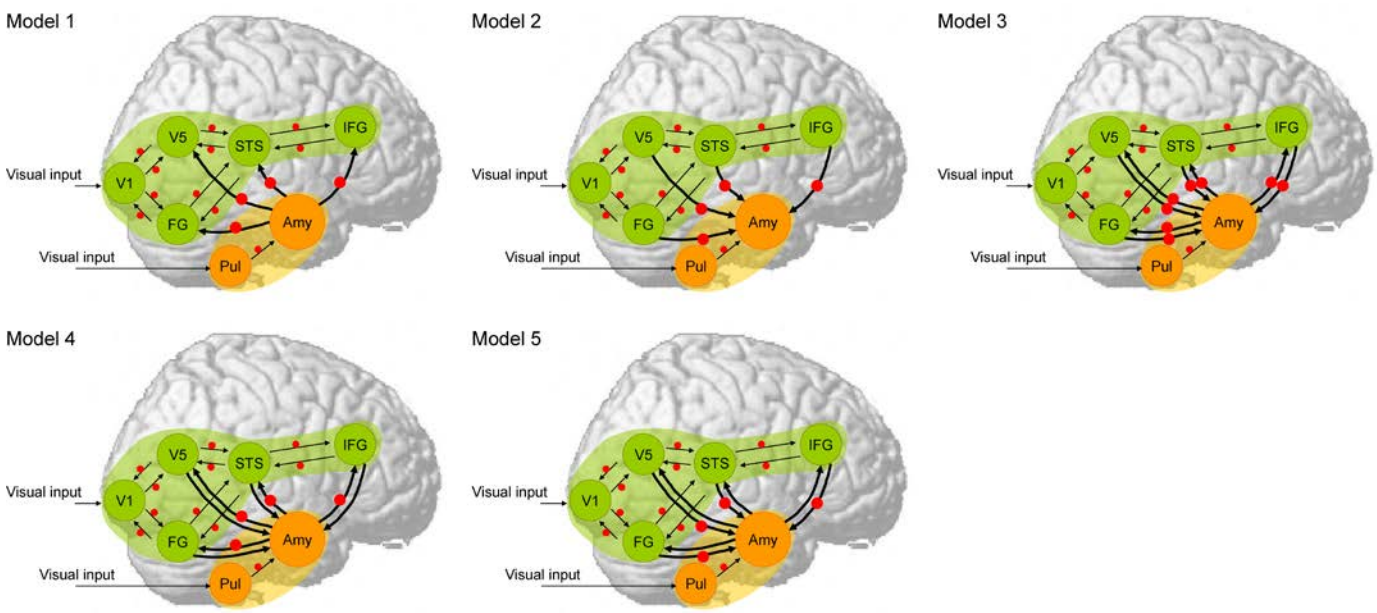

Figure 3.

Models of dynamic causal modeling. The analyzed brain regions are rendered on the spatially normalized brain. The arrows indicate intrinsic connections between brain regions; thick and thin arrows indicate manipulated and non-manipulated fixed connections, respectively. The red points indicate the modulatory effects of dynamic presentation. The subcortical and neocortical subnetworks, both of which have the same structure across models, are colored orange and green on the rendered brain, respectively. V1 = primary visual cortex; V5 = V5/middle temporal area; FG = fusiform gyrus; STS = superior temporal sulcus; IFG = inferior frontal gyrus; Amy = amygdala; Pul = pulvinar.

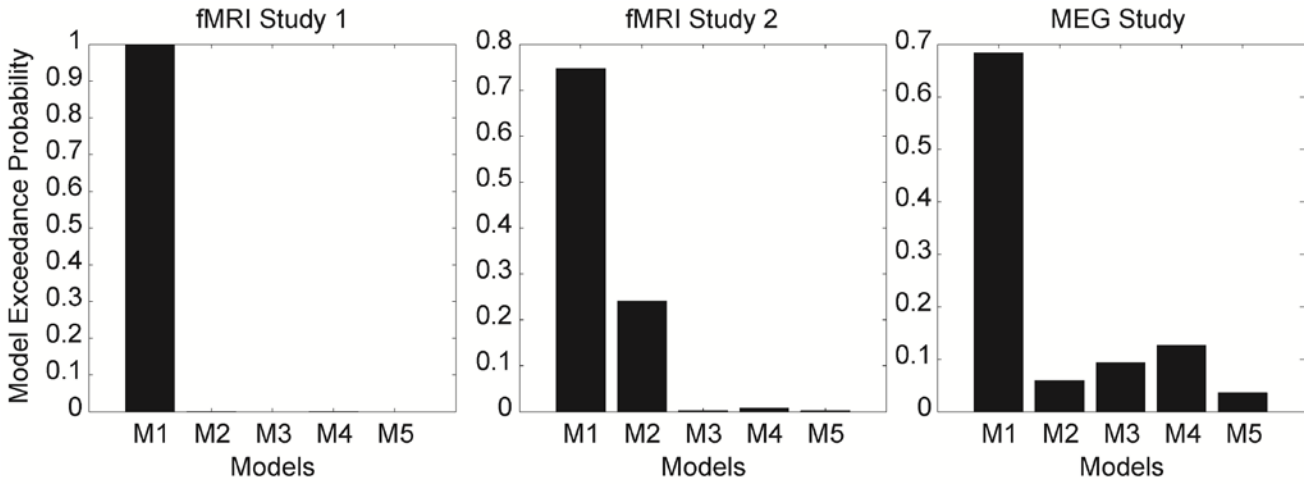

Figure 4.

Exceedance probabilities of the models in Bayesian model selection for the dynamic causal modeling analysis of functional magnetic resonance imaging (fMRI) study l (left), fMRI study 2 (middle), and magnetoencephalography (MEG) study (right).

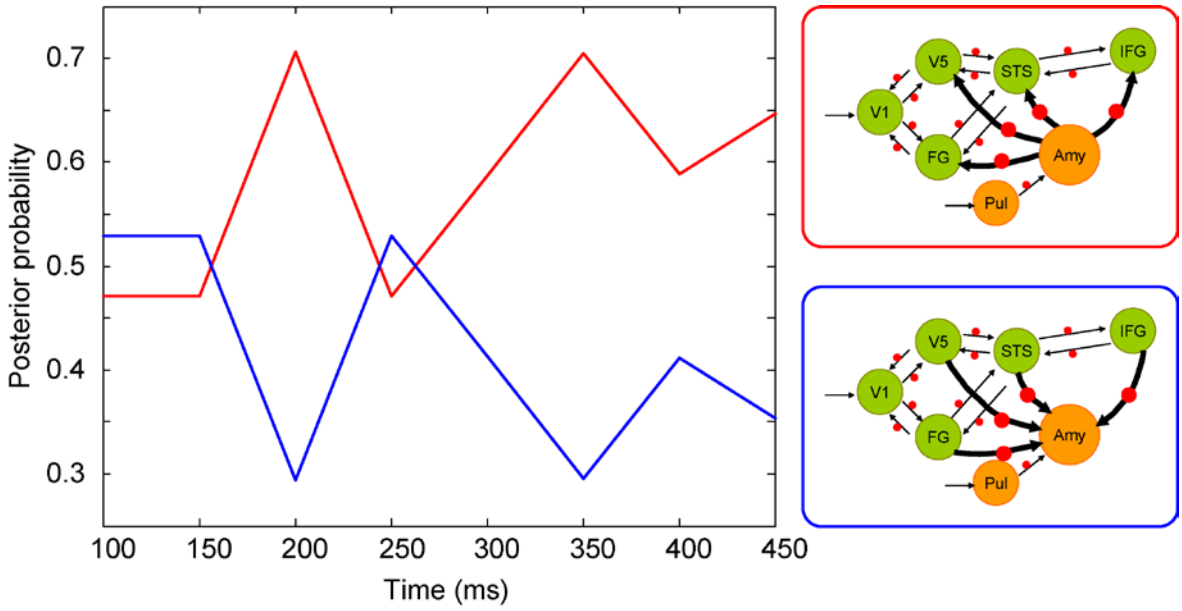

Figure 5.

The results of the increasing time-window analysis of dynamic causal modeling. Posterior probabilities in a random-effects Bayesian model selection of each time window (ranging from 100 to 450 ms in 50-ms increments) for "directional connectivity from the amygdala" (red) and "directional connectivity to the amygdala" (blue) models. V1 = primary visual cortex; V5 = V5/middle temporal area; FG = fusiform gyrus; STS = superior temporal sulcus; IFG = inferior frontal gyrus; Amy = amygdala; Pul = pulvinar.